

Electronic Supplementary Information

Nanoscale aggregates of porphyrin: red-shifted absorption, enhanced absorbance and phototherapeutic activity

Qihang Wu,^{ab} Rui Xia,^{ab} Chaonan Li,^{ab} Yite Li,^{ab} Tingting Sun,^{*a} Zhigang Xie^{*ab} and
Xiabin Jing^a

^a State Key Laboratory of Polymer Physics and Chemistry, Changchun Institute of Applied Chemistry, Chinese Academy of Sciences, Changchun, Jilin 130022, P. R. China

^b University of Science and Technology of China, Hefei 230026, P. R. China

*Corresponding authors

E-mail: suntt@ciac.ac.cn; xiez@ciac.ac.cn

Experimental Section

Materials and characterization

Pluronic F-127 was purchased from Shanghai yuanye Bio-Technology Co., Ltd. Cell viability (live-dead cell staining) assay kit was purchased from Jiangsu KeyGEN Biotechnology Co., Ltd. DSPE-PEG was purchased from Ponsure Biological Co., Ltd. DCFH-DA probe was purchased from Beyotime Biotechnology Co., Ltd. The other chemicals were used as obtained commercially. Analytical balance (XS105DU) and Rainin Pipettes from METTLER TOLEDO were used to quantify solid and liquid respectively. The absorption spectra were obtained from a TU-1901 UV-vis spectrophotometer (Persee). TEM and DLS results of NPs were determined by JEOL JEM-1011 electron microscope (acceleration voltage of 100 kV) and Malvern Zeta-sizer Nano. Powder X-ray diffraction results were obtained D8 Advance (Bruker, Germany). CLSM images were obtained from a Zeiss LSM 700 (Zurich, Switzerland).

Photothermal properties of TAPP-O NPs

TAPP-O NPs solutions at different concentrations ($10\text{-}50\ \mu\text{g mL}^{-1}$) were irradiated by a 685 nm laser ($0.5\ \text{W cm}^{-2}$) for 10 min. Then TAPP-O NPs were irradiated with laser of different power densities ($0.3, 0.5, 0.8$ and $1.0\ \text{W cm}^{-2}$). The photothermal response of TAPP-O NPs was recorded under laser irradiation for 10 min, and then the laser was turned off. To evaluate the photothermal stability, the temperature changes of TAPP-O NPs ($30\ \mu\text{g mL}^{-1}$) in aqueous solution were measured over 6 cycles of heating & cooling. The data above were recorded every 10 s by a thermocouple.

Intracellular detection of ROS

As a fluorescent ROS probe, 2',7'-dichlorofluorescein diacetate (DCFH-DA) was used to detect ROS generation in cells. First, human cervical carcinoma (HeLa) cells were treated with or without TAPP-O NPs for 4 h, and then irradiated with a 685 nm laser (0.2 W cm^{-2}) for 5 min followed by washing with phosphate-buffered saline (PBS) for 3 times. Subsequently, DCFH-DA was added, and cells were incubated for 20 min. After the media were removed, the cells were washed with PBS and observed via CLSM.

Cytotoxicity test

The cytotoxicity of TAPP-O NPs with or without laser irradiation was investigated by the classical 3-(4,5-dimethylthiazol-2-yl)-2,5-diphenyltetrazolium bromide (MTT) assay. HeLa cells were seeded into 96-well plates and cultured for 24 h. Then TAPP-O NPs at a series of concentrations ($0.4\text{-}1.0 \mu\text{g mL}^{-1}$) were added, and the cells were incubated for 4 h followed by irradiation with a 685 nm laser (0.2 W cm^{-2}) for 5 min. After incubation at $37 \text{ }^\circ\text{C}$ for 20 h, $20 \mu\text{L}$ of MTT solution (5 mg mL^{-1}) was added to each well. After 4 h, the media were removed and $150 \mu\text{L}$ of dimethyl sulfoxide (DMSO) was added into each well to dissolve the formazan crystals. Finally, the absorbance of each well at 490 nm was measured by a microplate reader.

Live-dead cell staining

HeLa cells were pretreated with PBS or TAPP-O NPs ($1.0 \mu\text{g mL}^{-1}$), and 4 h later, the cells were irradiated with a 685 nm laser (0.2 W cm^{-2}) for 5 min or not. After 20 h of incubation at $37 \text{ }^\circ\text{C}$, cells were stained with calcein-AM/propidium iodide (PI)

solution for 30 min at room temperature. Finally, the samples were imaged by a fluorescence microscope.

Cell apoptosis and necrosis assay

HeLa cells were pretreated with PBS or TAPP-O NPs ($1.0 \mu\text{g mL}^{-1}$), and 4 h later, the cells were irradiated with a 685 nm laser (0.2 W cm^{-2}) for 5 min or not. After incubation at $37 \text{ }^\circ\text{C}$ for 20 h, the cells were washed by PBS, then stained with Annexin-V-FITC and PI in binding buffer for 20 min. Finally, the apoptosis and necrosis assay was conducted by flow cytometer.

In vivo tumor inhibition effect

All animal experiments have been approved (Approved No. 202168) by the Academic Committee of Changchun Institute of Applied Chemistry, Chinese Academy of Sciences, and carried out according to the NIH guidelines for the care and use of laboratory animals (NIH publication No. 85-23 Rev. 1985). Female Kunming mice were injected subcutaneously with $100 \mu\text{L}$ of U14 cell suspension (containing 1×10^6 cells). When the tumor volumes reached about 200 mm^3 , the mice were randomly divided into 6 groups ($n=4$ for each group), namely PBS, PBS + 0.8 W cm^{-2} , 1.6 mg kg^{-1} , $0.4 \text{ mg kg}^{-1} + 0.2 \text{ W cm}^{-2}$, $1.6 \text{ mg kg}^{-1} + 0.2 \text{ W cm}^{-2}$ and $1.6 \text{ mg kg}^{-1} + 0.8 \text{ W cm}^{-2}$. Then intravenous injection of PBS or TAPP-O NPs solution (0.4 or 1.6 mg kg^{-1}) was conducted. After 12 h, the tumors of mice in PBS + 0.8 W cm^{-2} , $0.4 \text{ mg kg}^{-1} + 0.2 \text{ W cm}^{-2}$, $1.6 \text{ mg kg}^{-1} + 0.2 \text{ W cm}^{-2}$ and $1.6 \text{ mg kg}^{-1} + 0.8 \text{ W cm}^{-2}$ groups were exposed to a 685 nm laser at a power density of 0.2 or 0.8 W cm^{-2} for 10 min. After 14 days of treatment, mice were sacrificed, and the tumors and major organs

(heart, liver, spleen, lung and kidney) were collected for H&E staining.

Blood biochemistry assay

After 14 days of treatment, the mice in PBS and $1.6 \text{ mg kg}^{-1} + 0.8 \text{ W cm}^{-2}$ groups were sacrificed, and their blood was collected for biochemistry assay. The liver & kidney function markers were analyzed by an automatic biochemical analyzer. Besides, the whole blood test was carried out by the automatic blood cell analyzer.

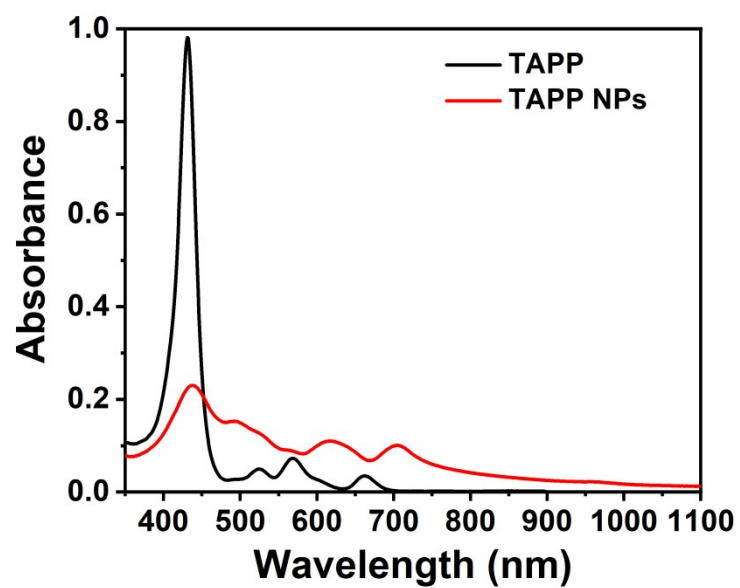


Fig. S1 Absorption spectra of TAPP in THF and TAPP NPs in water at the same concentration ($2.7 \mu\text{g mL}^{-1}$).

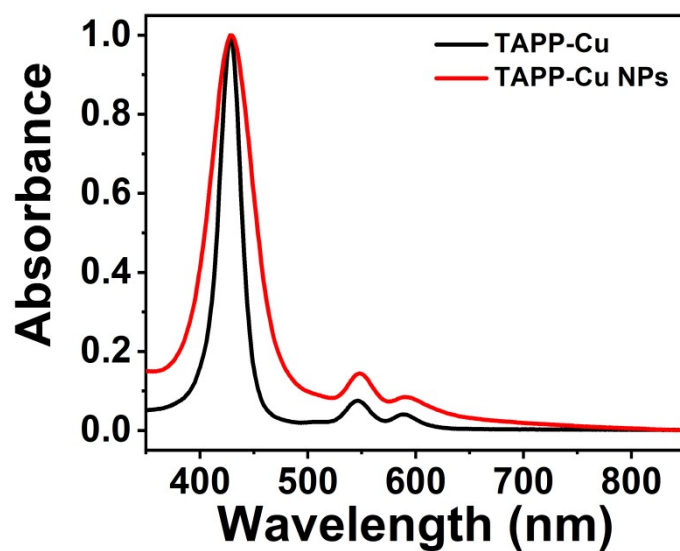


Fig. S2 The normalized absorption spectra of TAPP-Cu in THF and TAPP-Cu NPs in water.

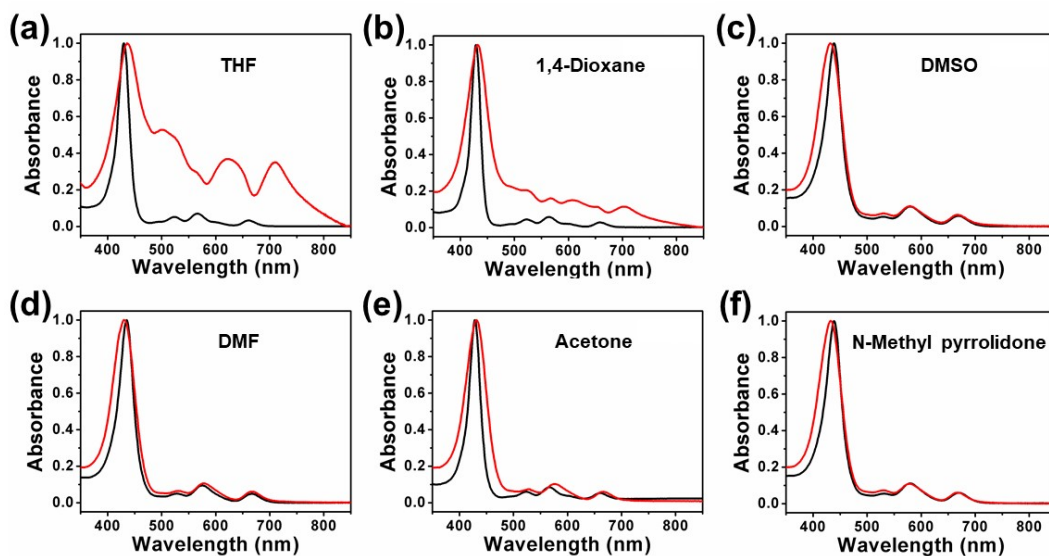


Fig. S3 The normalized absorption spectra of TAPP in different organic solvents (black lines) and corresponding NPs in water (red lines). (a) Tetrahydrofuran (THF). (b) 1,4-Dioxane. (c) Dimethyl sulfoxide (DMSO). (d) N,N-Dimethylformamide (DMF). (e) Acetone. (f) N-Methyl pyrrolidone.

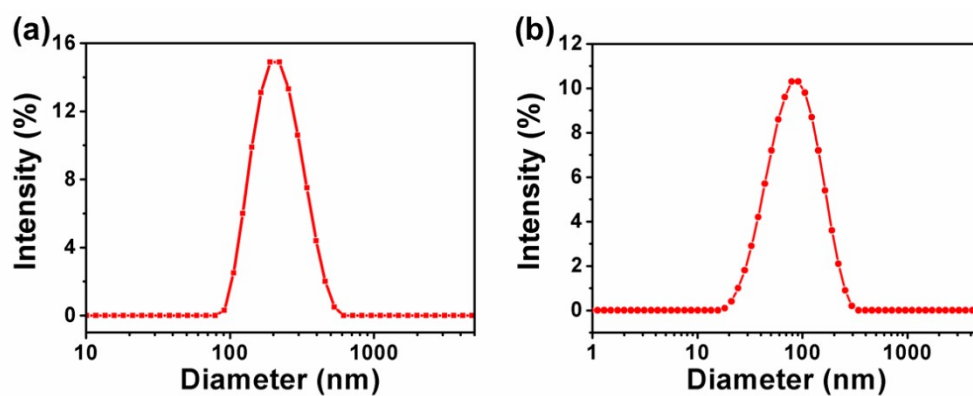


Fig. S4 DLS results of TAPP-O NPs (a) and TAPP-D NPs (b).

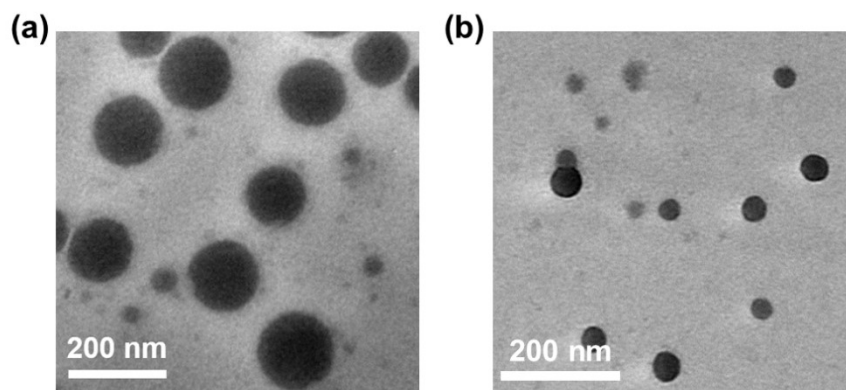


Fig. S5 TEM images of TAPP-O NPs (a) and TAPP-D NPs (b).

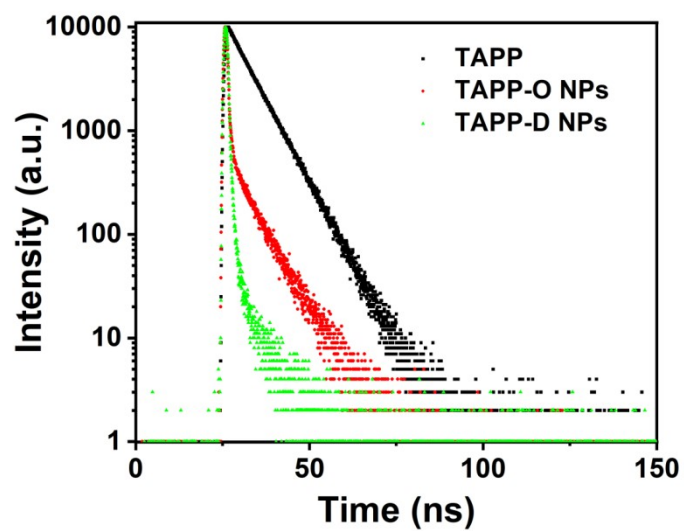


Fig. S6 The fluorescence decay curves of TAPP, TAPP-O NPs and TAPP-D NPs ($\lambda_{\text{ex}}=455$ nm).

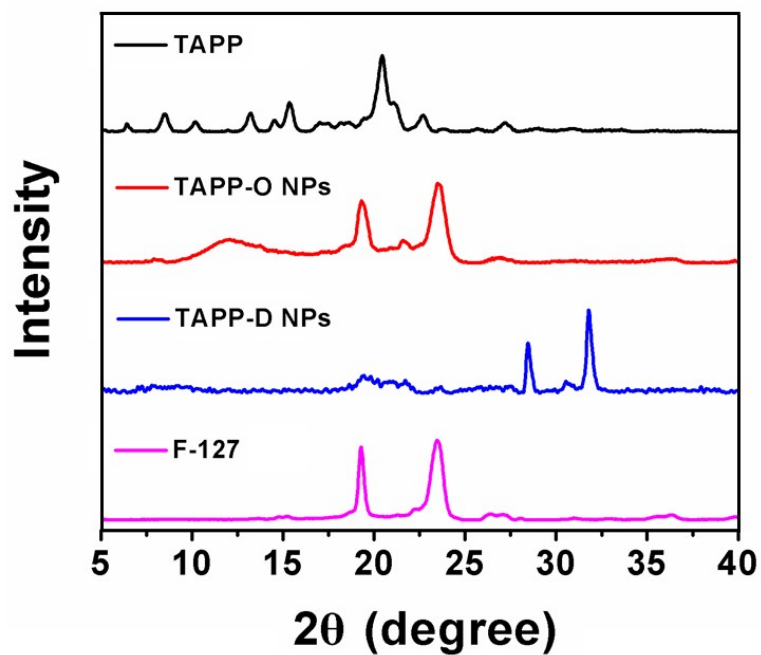


Fig. S7 PXRD patterns of TAPP, TAPP-O NPs, TAPP-D NPs and F-127.

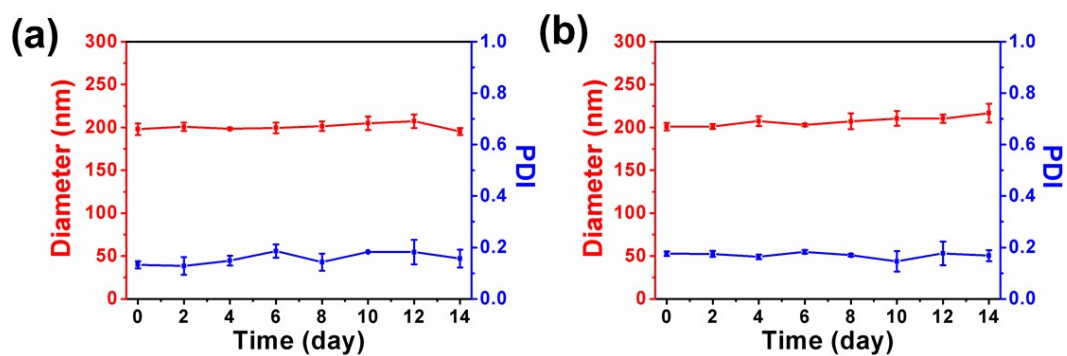


Fig. S8 Size and PDI variations of TAPP-O NPs in water (a) and PBS (b) containing 10% fetal bovine serum.

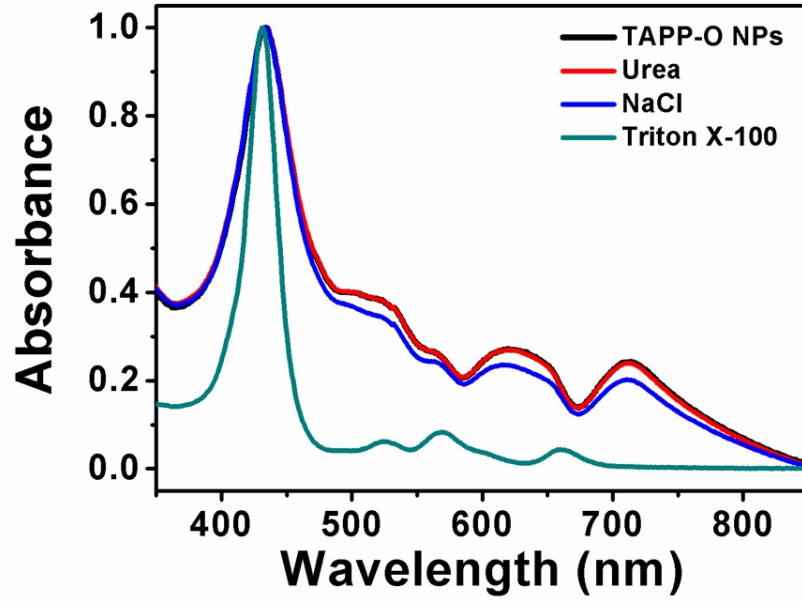


Fig. S9 Absorption spectra of TAPP-O NPs in water and treated with urea, NaCl or Triton X-100.

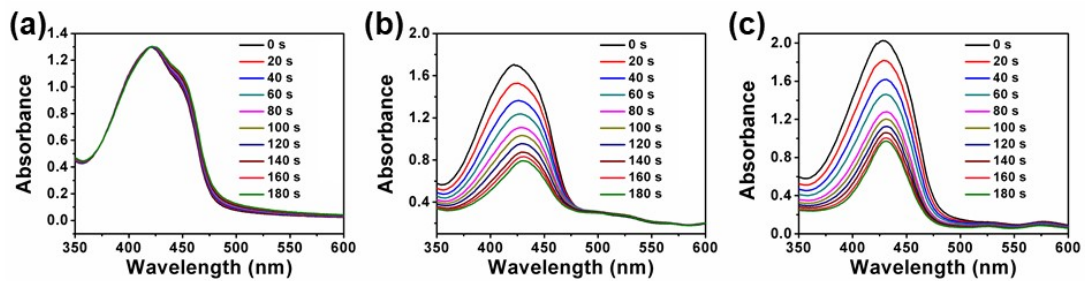


Fig. S10 The absorption spectra changes of DPBF induced by ROS generation from water (a), TAPP-O NPs (b) and TAPP-D NPs (c) with laser irradiation.

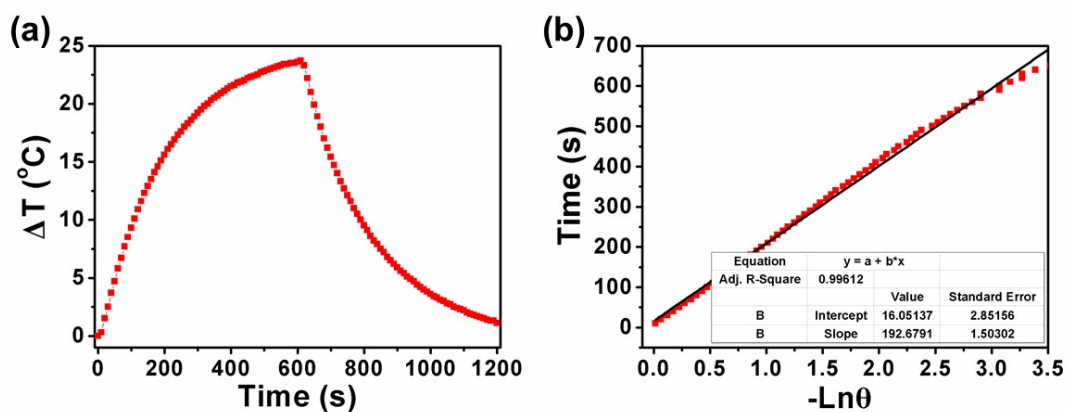


Fig. S11 (a) Photothermal response of TAPP-O NPs with laser irradiation, and the laser was turned off 600 s later. (b) The relationship between cooling period of time and the negative natural logarithm of temperature changes.

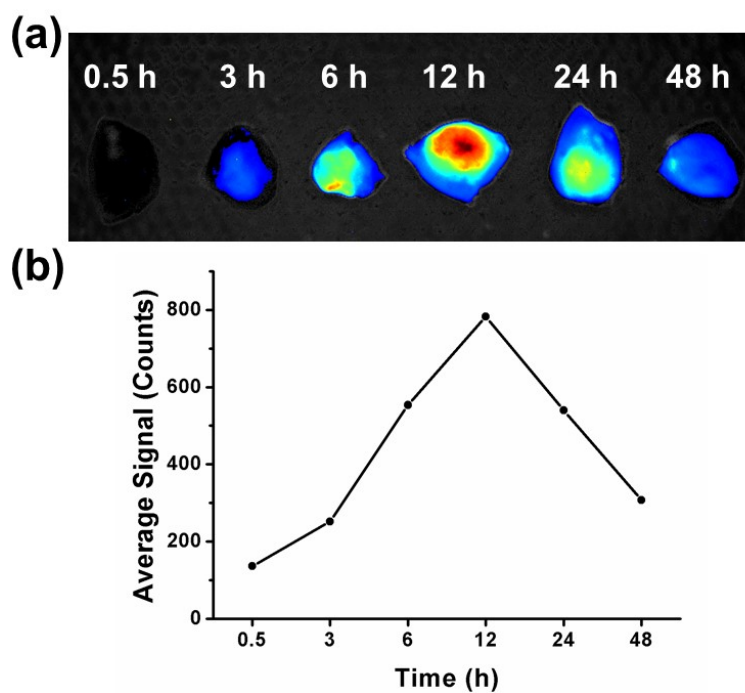


Fig. S12 Ex vivo fluorescence images (a) and the fluorescence intensity (b) of tumors after intravenous injection of TAPP-O NPs for different times.

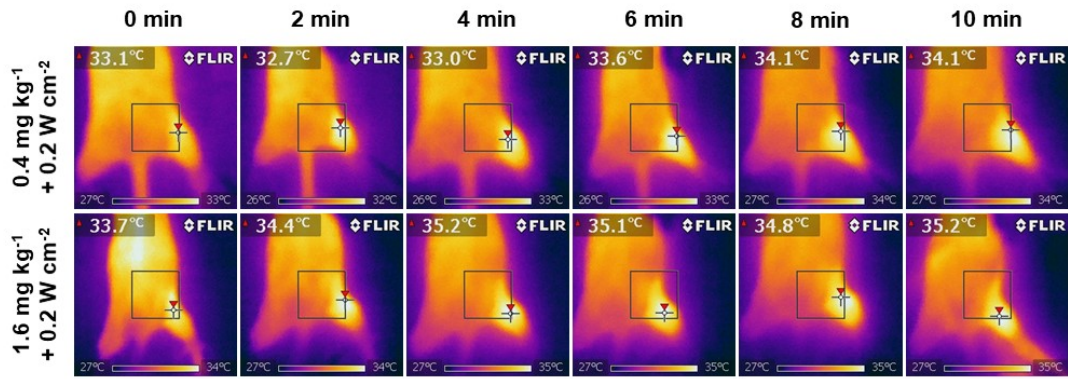


Fig. S13 Infrared photothermal images of tumor sites of U14 tumor-burdened mice intravenously injected with TAPP-O NPs (0.4 or 1.6 mg kg⁻¹) and irradiated with a 685 nm laser (0.2 W cm⁻²).

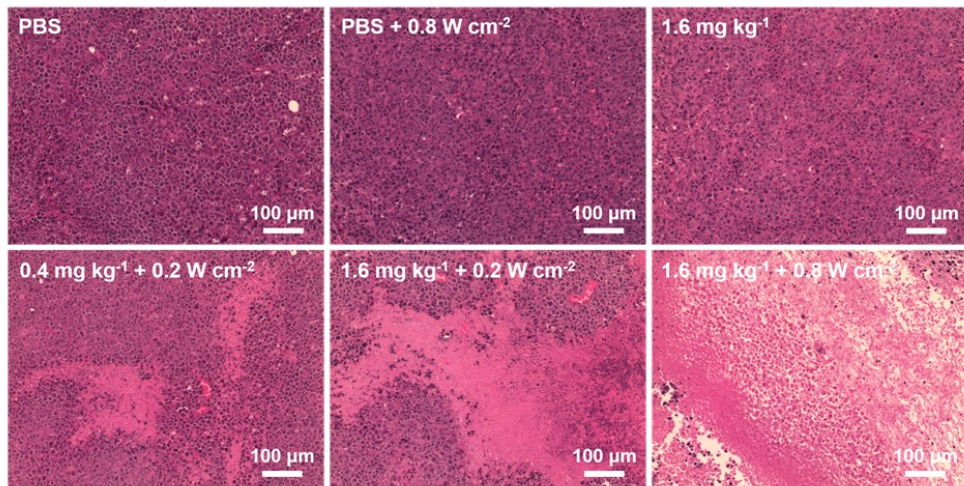


Fig. S14 H&E staining of tumor sections harvested from the mice in each group after treatments.

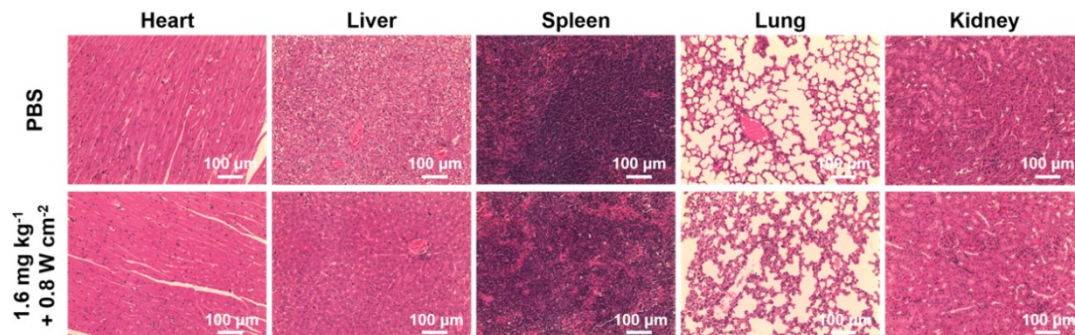


Fig. S15 H&E staining images of the main organs (heart, liver, spleen, lung and kidney) from mice in PBS and 1.6 mg kg⁻¹ + 0.8 W cm⁻² groups.

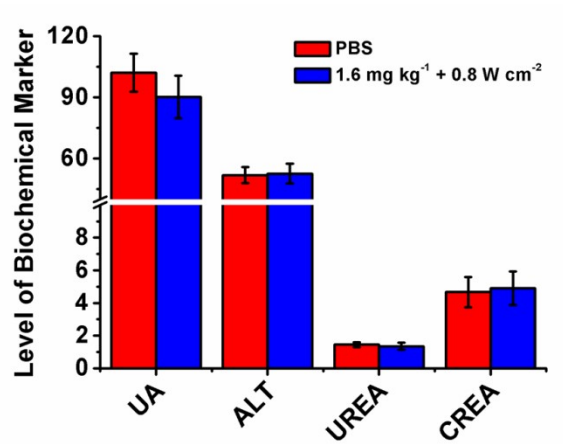


Fig. S16 Serum biochemical analysis of kidney and liver function parameters of the mice in PBS and 1.6 mg kg⁻¹ + 0.8 W cm⁻² groups.

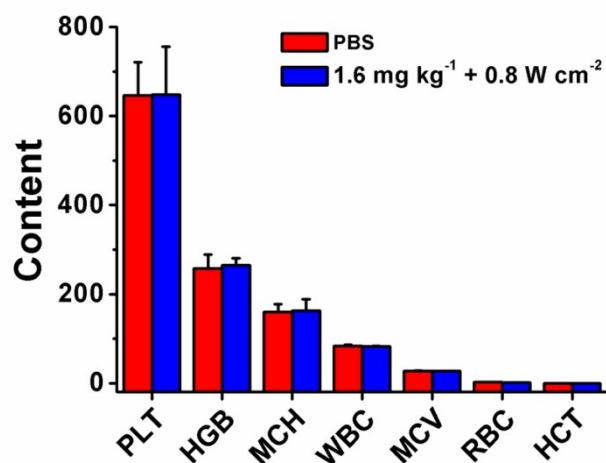


Fig. S17 Hematology data of the mice in PBS and 1.6 mg kg⁻¹ + 0.8 W cm⁻² groups.